Flexible and Printed Electronics

PAPER

Efficient flexible perovskite solar cells based on a polymer additive

Yangjie Lan[1], Yang Wang[1] and Yanlin Song

Key Laboratory of Green Printing, Institute of Chemistry Chinese Academy of Sciences, Beijing 100190, People's Republic of China
[1] These authors contributed equally to this work.

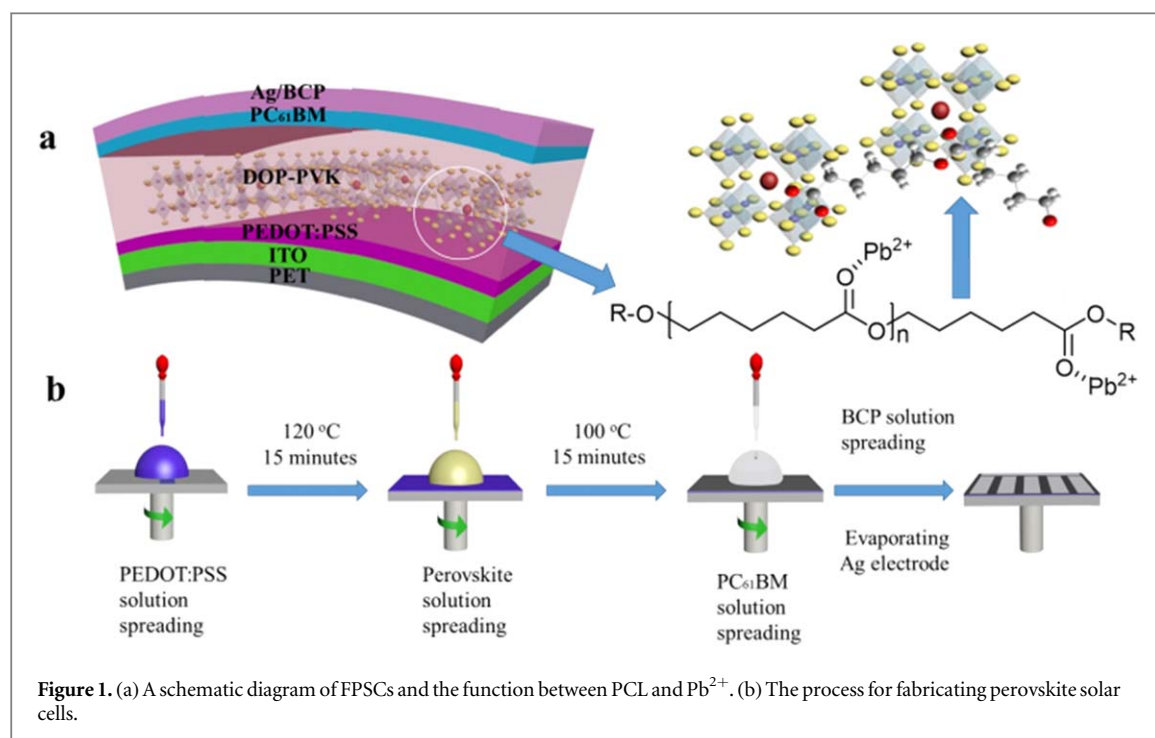E-mail: wangyang@iccas.ac.an and ylsong@iccas.ac.cn

Abstract

The rapid development of flexible perovskite solar cells (FPSCs) has attracted more and more attention. The application of FPSCs is largely in thrall to the fragility of perovskite crystals and quality of perovskite films caused by the inherent nature and uncertain grain size of perovskite. A polymer additive as an efficient strategy is utilized to restrict the fragility and improve the durability of FPSCs. In this work, we use polycaprolactone (PCL) as a polymer additive to achieve the grain boundary regulation (improving the grain size) and the desirable mechanical strength of FPSCs. A champion device based on glass/indium tin oxide (ITO) achieves high photoelectric conversion efficiency (PCE) (14.49%), which is ∼37.7% higher than that of the pristine film (10.52%). While the efficiency of FPSCs also retains 9.11%, which is 90% of the initial PCE (10.12%) after 300 bending cycles. Importantly, the PCL as a polymer additive shows great potential for future applications in wearable electronics.

1. Introduction

Perovskite material ($CH_3NH_3PbI_3$) is a hybrid inorganic–organic direct-bandgap semiconductor that shows great promise in light absorbance, especially as a light harvester for perovskite solar cells [1–6]. High-quality perovskite thin films are formed at low temperature, which shows great advances for fabricating facile solar cells [7–11]. According to the latest reports, perovskite solar cells have revolutionized thin film photovoltaics as the efficiency reached 25.2% (2019) based on the glass substrates. However, flexible perovskite solar cells (FPSCs) have been considered as a promising photovoltaic technology due to their intrinsic advantages, such as their light weight and bendability, which make them very convenient for transportation, installation and integration with architecture and wearable electrical devices [12–15]. Many researchers working on FPSCs (the electron transport layer and the hole transport layer) have made efforts to improve the flexibility and photoelectric properties of the FPSCs [16–19]. However, the inherent nature and uncertain grain size of perovskite, the fragility of perovskite crystals and the quality of the perovskite itself in the perovskite films can seriously decrease the

flexibility and power conversion efficiency and restrict the application of FPSCs [20, 21]. Fortunately, the polymer additive as an effective and viable strategy overcomes these disadvantages and enhances the performance of FPSCs [22–24]. Polycaprolactone (PCL) is an adhesive with good flexibility, hydrophobicity and a functional carbonyl group which can efficiently improve the flexibility of perovskite films and achieve the grain boundary regulation with large grain size, less defects and high quality of perovskite films [25–27].

In this work, we utilize PCL as a polymer additive to resolve the disadvantages of FPSCs. In figure 1(a), PCL as an additive improves the flexibility of perovskite films, and the function of the carbonyl (C=O) and Pb^{2+} bond [11, 28] can ensure the uniform coverage of perovskite, which avoids the defects caused by uncertain grain size distribution and achieves the grain boundary regulation. Finally, the PCL makes the perovskite films composed of small grains (less than 200 nm) convert into high-quality perovskite films with free pinholes, less defects and large grains (more than 400 nm, up to two-fold than the pristine film). The photoelectric conversion efficiency (PCE) of perovskite solar cells (PSCs) based on glass/indium tin

Figure 1. (a) A schematic diagram of FPSCs and the function between PCL and Pb^{2+}. (b) The process for fabricating perovskite solar cells.

oxide (ITO) achieves high a PCE up to 14.49%, which is ∼37.7% higher than that of the pristine film (10.52%). After 300 bending cycles, the efficiency of FPSCs also retains 90% of the initial PCE (10.12%).

2. Materials and methods

2.1. Materials
ITO-coated glass (sheet resistance is less than 10 ohm/sq, transmittance is more than 85%) and ITO-coated polyethylene terephthalate (PET) were purchased from Shenzhen Huanan Xiangcheng Technology Co., Ltd. Methylamine iodide (CH_3NH_3I, 99.0%), lead (II) iodide (PbI_2, 99.0%), [6,6]-phenyl-C_{61}-butyric acid methyl ester ($PC_{61}BM$), bathocuproine (BCP, 96.0%) were purchased from Xi'an Baolaite. Poly(3,4-ethlene-dioxyl-enethiophene):poly(styrene sulfonate) (PEDOT:PSS) aqueous solution (Al 4083) was purchased from Heraeus. N,N-dimethylformamide (DMF, AR), PCL (medical grade, M.W. 40 000–160 000), dimethyl sulfoxide (DMSO, AR), chlorobenzene (CB, anhydrous, 99.8%) and isopropanol were purchased from Sigma-Aldrich. Acetone (AR) and ethanol (AR) were purchased from Beijing Chemical Works. Ag (99.99%) was purchased from China New Metal Materials Technology Co., Ltd.

2.2. Substrate preparation
Flexible PET/ITO substrates and glass/ITO substrates have been etched by zinc powder and hydrochloric acid (2 mol l^{-1}). These substrates are washed with deionized water, acetone, ethanol and isopropanol in ultrasonic ink for 20 min and dried with nitrogen gas. The flexible substrate (PET/ITO) is adhered to the glass (1.5 cm × 1.5 cm) by PDMS (polydimethylsiloxane).
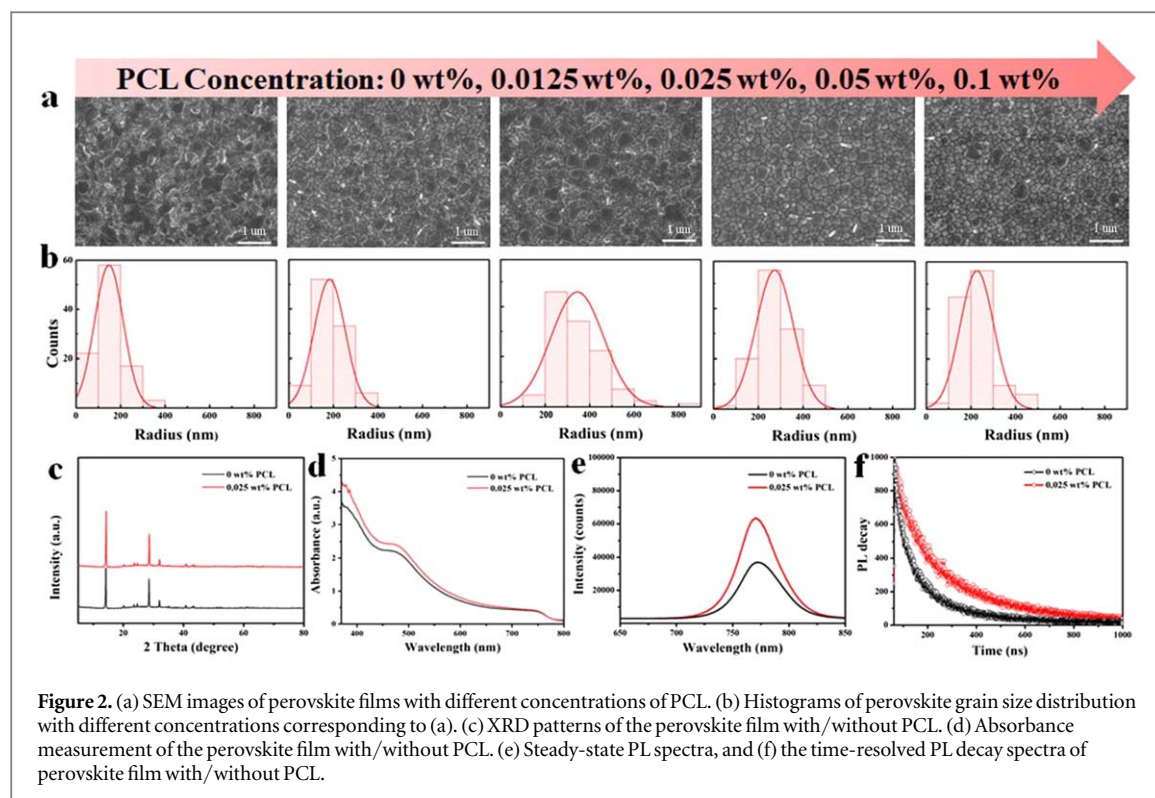
2.3. Perovskite precursor solution
For the perovskite precursor solution, 0.461 g PbI_2 and 0.159 g methylammoniumiodide (molar ratio of 1:1) are dissolved in l mL mixed solvent of anhydrous DMF and anhydrous DMSO (volume ratio 4:1). PCL is dissolved with the corresponding weight ratio of perovskite (0 wt%, 0.0125 wt%, 0.025 wt%, 0.05 wt% and 0.1 wt%).

2.4. Device fabrication
The prepared substrates are treated with O_2-plasma for 15 min. Then, the PEDOT:PSS is spin coated on the substrates at 4000 rpm for 40 s and annealed at 120 °C for 15 min in ambient air. Next, the substrates are transferred into the glove box. The $CH_3NH_3PbI_3$ precursor solution with PCL (0 wt%, 0.0125 wt%, 0.025 wt%, 0.05 wt%, 0.1 wt%) is deposited onto the substrates by spin coating at 4000 rpm for 40 s. Then, chlorobenzene (120 ul) is quickly dropped onto the substrates in the last 25 s of the spin coating. After annealing at 100 °C for 15 min, $PC_{61}BM$ and BCP are spin coated on these substrates at 1000 rpm and 5000 rpm for 60 s, respectively. Finally, a Ag electrode (∼70 nm) is deposited on the BCP layer by thermal evaporation. We obtained the fabricated PSCs with the glass or PET/ITO/PEDOT:PSS/perovskite/$PC_{61}BM$/BCP/Ag structure. The FPSCs with the PET/ITO/PEDOT:PSS/perovskite/$PC_{61}BM$/BCP/Ag structure and a schematic diagram are shown in figures 1(a) and (b).

Figure 2. (a) SEM images of perovskite films with different concentrations of PCL. (b) Histograms of perovskite grain size distribution with different concentrations corresponding to (a). (c) XRD patterns of the perovskite film with/without PCL. (d) Absorbance measurement of the perovskite film with/without PCL. (e) Steady-state PL spectra, and (f) the time-resolved PL decay spectra of perovskite film with/without PCL.

3. Characterization

The morphology of the perovskite films was measured by a field-emission scanning electron microscope (SEM, JEOL, JSM-7500F, Japan). The x-ray diffraction (XRD) patterns were measured by a D8 FOCUS powder diffractometer (Bruker). Absorbance spectra were measured by a UV-vis spectroscopy photometer (Perkin Elmer Lambda 750). The J–V curves were measured under AM 1.5G solar irradiation at 100 mW cm^{-2} (Enli Tech, Class AAA solar simulator). The external quantum efficiency (EQE) is the measured illumination with monochromatic xenon-lamp (Enli Tech, Class AAA solar simulator, QE-mini) at the range of 300 nm–850 nm. Repeated bending cycles were measured by a custom-made machine, providing the momentum by a stepper motor.

4. Results and discussion

The effect of PCL as a polymer additive with the functional carbonyl group on the perovskite grain size was verified by comparing the grain size evolution of the MAPbI$_3$ films with the change in PCL concentrations (from 0 wt%, 0.0125 wt%, 0.025 wt%, 0.05 wt%, to 0.1 wt%). The PCL is expected to uniformly trigger heterogeneous nucleation over the perovskite precursor film to improve the grain size. Figure 2(a) shows the SEM images of perovskite films with different PCL concentrations (the SEM images and thicknesses of perovskite films are shown in figures S1 and S2 (available online at stacks.iop.org/FPE/5/014001/mmedia). Based on the statistical method, the average

grain size has been obviously increased when the PCL concentration reaches 0.025 wt% compared with the pristine film, which also avoids the pinholes and defects. The grain size distributions of perovskite films with PCL are summarized in figure 2(b). Most of the grain sizes with PCL concentrations (from 0.0125 wt-%, 0.025 wt%, 0.05 wt%, to 0.1 wt%) increased, with their average grain size/pristine ratio reaching 1.2, 2.3, 1.8 and 1.4, respectively. The average grain size with 0.025 wt% PCL is much larger than that of the pristine film (up to 2.3-fold). Based on the above, these results show that the PCL polymer additive can improve the quality of perovskite films and grain sizes, benefiting from a reduction in the surface area of the grain boundaries.

To gain a deeper insight into the effect of PCL on the formation of crystal, XRD measurement has been employed to investigate the difference between the pristine film and perovskite with PCL. As shown in figure 2(c), the dominating peaks of the pristine film and perovskite with PCL appear at 14.08° and 28.36°, corresponding to the (110) and (220) planes of the tetragonal perovskite structure of MAPbI$_3$. It indicates that the PCL as a polymer additive does not influence the crystalline structure. However, the diffraction intensity of the perovskite with PCL is stronger than the pristine perovskite, which indicates that the perovskite film with PCL achieves high quality. Moreover, when comparing the full-width at half-maximum (FWHM) of the (110) reflection, we attribute the larger crystal size to the effect of PCL on crystal growth because the carbonyl groups in the PCL form an intermediate adduct with Pb^{2+} [11, 28]. As shown in
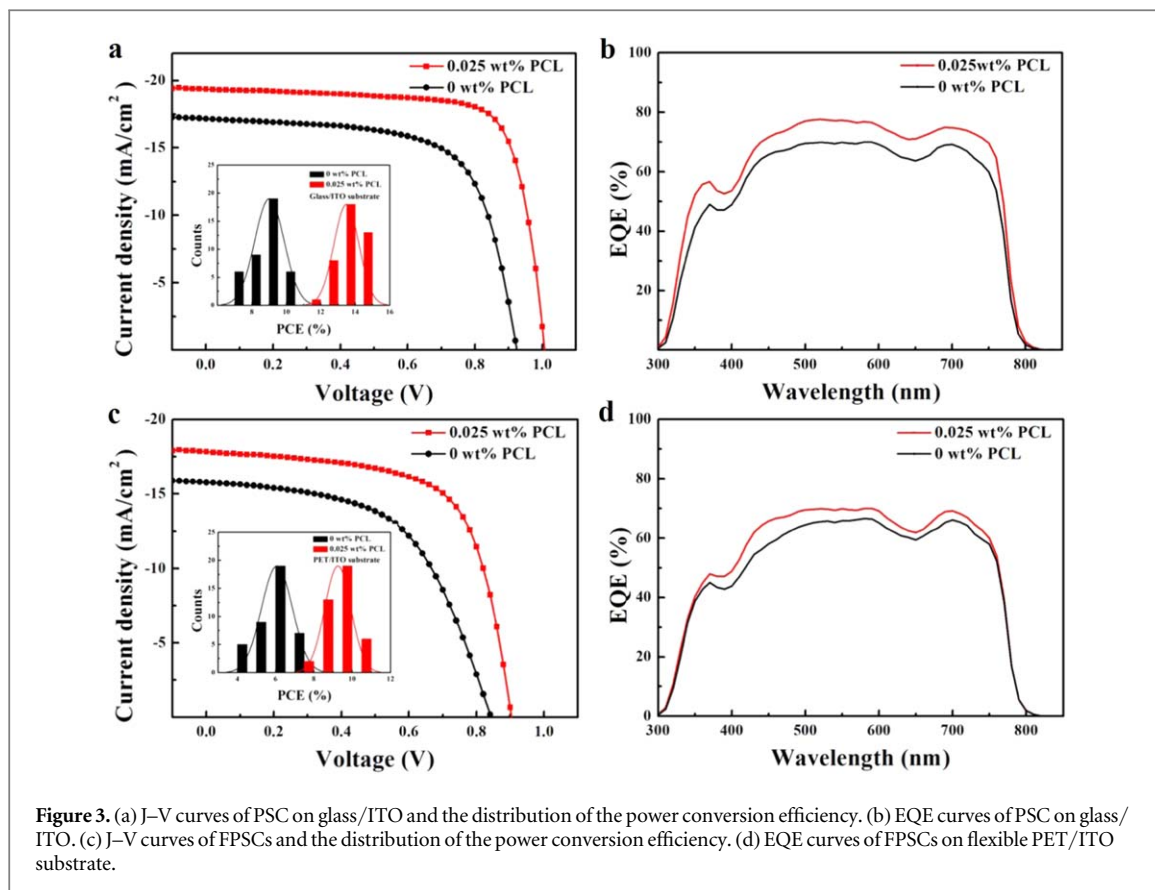
Figure 3. (a) J–V curves of PSC on glass/ITO and the distribution of the power conversion efficiency. (b) EQE curves of PSC on glass/ITO. (c) J–V curves of FPSCs and the distribution of the power conversion efficiency. (d) EQE curves of FPSCs on flexible PET/ITO substrate.

Table 1. The J–V characteristic curves of the PSCs measured under simulated standard AM 1.5G solar illumination.

Samples		V_{OC} (V)	FF (%)	J_{sc} (mA cm^{-2})	PCE (%)
Glass/ITO	0 wt%	0.92	66.64	17.15	10.52
	0.025 wt%	1.01	74.14	19.35	14.49
PET/ITO	0 wt%	0.83	55.34	15.50	7.12
	0.025 wt%	0.91	61.07	18.21	10.12

figure 2(d), we also measure the UV-vis spectra to evaluate the influence of PCL on the perovskite film. It clearly shows that the absorption of perovskite film with 0.025 wt% PCL is higher than the pristine film in the range of visible light. In addition, the quality of the perovskite film with PCL is better than the pristine film.

Furthermore, the steady-state photoluminescence (PL) spectroscopy is measured, as shown in figure 2(e). These perovskite films are prepared on the O_2-plasma cleaned glass substrates. The perovskite emission peak is located at ~770 nm, and the emission peak intensity of the perovskite film with 0.025 wt% PCL is higher than the others with the different concentrations (as discussed in figure S3), which indicates that PCL is beneficial for reducing the surface defects and enhancing the crystallinity of perovskite film [23]. This result also corresponds to the absorption spectra of perovskite films. To quantify the PL lifetime of the perovskite films with PCL, the time-resolved PL decay of perovskite films on glass has been measured, as shown

in figure 2(f). We fit the data with a global bi-exponential model, and the detailed fitted PL lifetimes (τ_1, τ_2 and τ) are collected; the PL decay curves are fitted to a bi-exponential rate law [11, 25]:

$$y = A_1 \exp(-t/\tau_1) + A_2 \exp(-t/\tau_2) + y_0 \qquad (1)$$

where A_1 and A_2 are the relative amplitude, τ_1 is the lifetime for fast recombination related to the surface recombination and τ_2 is the lifetime of non-radiative decay, which is related to bulk recombination. The slowest is the non-radiative decay, leading to longer-living charge carriers and longer charge carrier diffusion length. The PL decay of perovskite films is shown in figure 2(f), revealing a much faster decay for the pristine film than the perovskite film with PCL. The decay is attributed mainly to trap-assisted recombination at defects. The perovskite film with PCL exhibits fast and slow phase lifetimes of $\tau_1 = 50.82$ ns (fraction $A_1 = 0.73$) and $\tau_2 = 419.81$ ns (fraction $A_2 = 0.27$), respectively. In contrast, the pristine film gives $\tau_1 = 23.85$ ns (fraction $A_1 = 0.51$) and
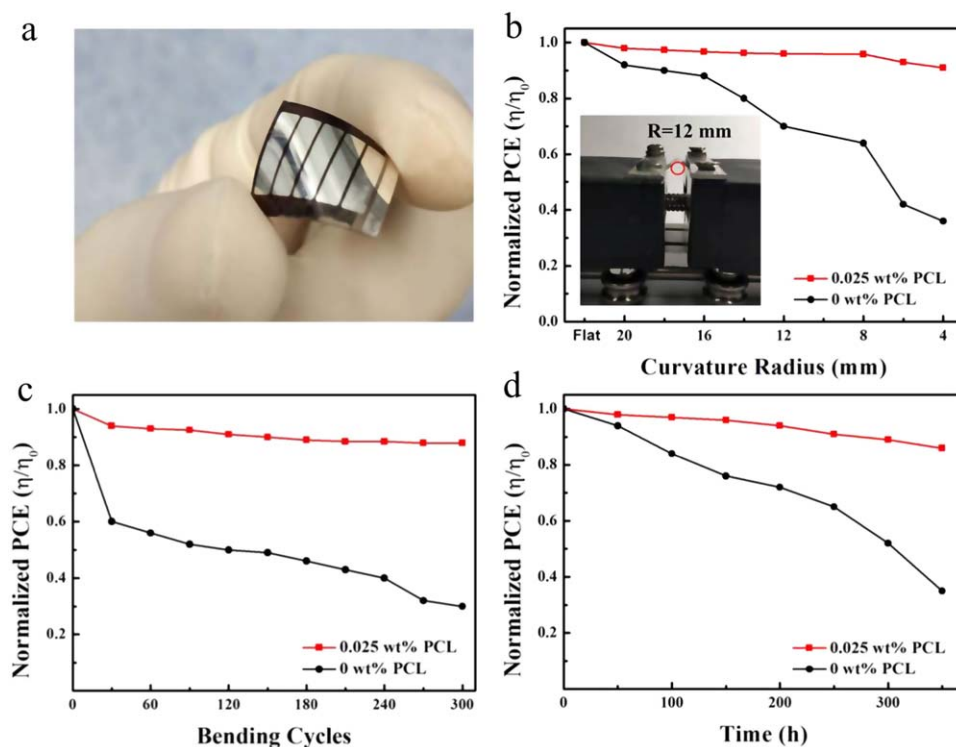
Figure 4. (a) An image of the FPSCs. (b) The normalized PCE versus different curvature radii of the FPSCs. (c) The normalized PCE versus cycle times of the FPSCs. (d) Stability measurement of the FPSCs.

$\tau_2 = 174.28$ ns (fraction $A_2 = 0.49$), respectively. The result indicates that the perovskite film with PCL has a higher crystal quality and lower defect concentration, resulting in the good interfacial charge separation and superior electronic quality, consistent with the higher open-circuit voltage (V_{OC}), as shown in figures 3(a) and (c).

The advantages of photoelectric performance and the distribution of power conversion efficiency for PSCs with PCL are investigated by the J–V curves based on glass/ITO and PET/ITO substrates under simulated standard AM 1.5G solar illumination with a light intensity of 100 mW cm^{-2} from 1.1 V to −0.1 V at the ratio of 0.02 V s^{-1} and the delay time (30 ms), as shown in figures 3(a) and (c). Furthermore, the inset images (figures 3(a) and (c)) are the distribution of PCE based on 40 devices at the PCL concentrations of 0 wt% and 0.025 wt% on the substrates of glass and PET, respectively. Other J–V curves with different concentrations on the glass substrates are shown in figure S4. Figure S5 shows the PSC performance statistics of the short-circuit current density (J_{sc}), V_{oc}, fill factor (FF) and PCE with different concentrations of PCL. The champion devices on glass/ITO and PET/ITO at the concentrations of 0 wt% and 0.025 wt% are summarized in table 1.

The device without PCL based on the glass/ITO obtains a PCE of 10.52%, J_{SC} of 17.15 mA cm^{-2}, V_{OC} of 0.92 V and FF of 66.64%, while the photoelectric performance of the device with PCL on the glass/ITO as the champion device obtains a higher PCE of 14.49%, J_{SC} of 19.35 mA cm^{-2}, V_{OC} of 1.01 V and FF of 74.14%. Compared with the pristine film, the PCE of the PSCs with PCL increases 37.7% from 10.52% to 14.49%. The EQE of the PSCs with PCL is higher than that of the pristine film, which demonstrates that the PSCs with PCL generate more electrons (figure 3(b)). In comparison with the pristine film, the V_{OC} of the device with PCL is obviously improved, which is attributed to the large grain size and high quality of perovskite film with fewer surface defects and lower defect-induced recombination caused by the carbonyl function of PCL. Based on the good performances of PCL, we utilize the PCL to fabricate the flexible PSCs. The pristine FPSCs obtain a PCE of 7.12%, a J_{SC} of 15.5 mA cm^{-2}, a V_{OC} of 0.83 V and an FF of 55.34%. The champion FPSCs with PCL obtains a higher PCE of 10.12%, J_{SC} of 18.21 mA cm^{-2}, V_{OC} of 0.91 V and FF of 61.07%. Compared with the pristine FPSCs, the performances of the FPSCs with PCL are obviously improved, as shown in figure 3(c). In figure 3(d), the EQE spectra demonstrate the high quantum conversion efficiency of the device with PCL throughout the entire wavelength range.

The properties of flexibility and durability under bending cycles are very important to the application of the flexible PSCs. Based on this, the stability versus the mechanical bending of FPSCs has been measured. Figure 4(a) shows the image of the FPSCs with PCL. We measure the bending resistance of the devices under a series of different curvature radii from 20 mm to 4 mm. In figure 4(b), the stability of the devices for

bending resistance has been recorded under every radius after 10 cycles. The PCE stability of the devices without PCL goes sharply down to 36% of the initial PCE with 4 mm curvature radius, which is attributed to the brittleness of the perovskite.

Compared with the pristine FPSCs, the stability of the FPSCs with PCL is maintained above 90% under the radius from 20 mm to 4 mm, which is beneficial for improving the flexibility of FPSCs by adding PCL. The bending cycles and device lifetime measurements of FPSCs w/wo-PCL have been carried out, as shown in figures 4(c) and (d). After 300 bending cycles, there is no obvious crack in the perovskite film (see figure S6). Moreover, the PCE of FPSCs with PCL is retained up to 90%, which is better than the pristine film (32%). Furthermore, the PCE of the FPSCs with PCL retains the 88% after continuous illumination (350 h) compared to the pristine. These results further indicate that PCL as a polymer additive efficiently promotes the flexibility and stability of FPSCs.

5. Conclusion

In this work, we use PCL as a polymer additive to improve the flexibility of perovskite film and regulate the grain boundary, which can avoid the defects due to uncertain grain size distribution and can increase the grain size as well as the quality of the perovskite film. A champion device based on glass/ITO achieves a PCE up to 14.49%, which is ~37.7% higher than that of the pristine perovskite (10.52%). After 300 bending cycles, the efficiency of the FPSCs retains 90% of the initial PCE (10.12%). The results show that PCL is a promising material for improving the performance of devices, which also provides a simple way to improve the flexibility of perovskite devices.

Acknowledgments

ORCID iDs

Yanlin Song ● https://orcid.org/0000-0002-0267-3917

References

[1] Kojima A, Teshima K, Shirai Y and Miyasaka T 2009 *J. Am. Chem. Soc.* **131** 6050–1
[2] Burschka J, Pellet N, Moon S J, Humphry-Baker R, Gao P, Nazeeruddin M K and Gratzel M 2013 *Nature* **499** 316–9
[3] Lund P D, Halme J, Hashmi G, Asghar I and Miettunen K 2018 *Flexible Print. Electron.* **3** 013002
[4] Jiang F Y *et al* 2016 *Adv. Funct. Mater.* **26** 8119–27
[5] Wang Y, Li M Z, Zhou X, Li P W, Hu X T and Song Y L 2018 *Nano Energy* **51** 556–62
[6] Wang Y, Wang P, Zhou X, Li C, Li H Z, Hu X T, Li F Y, Liu X P, Li M Z and Song Y L 2018 *Adv. Energy Mater.* **8** 1702960
[7] Ostfeld A E and Arias A C 2017 *Flexible Print. Electron.* **2** 013001
[8] Bi C, Chen B, Wei H T, DeLuca S H and Huang J 2017 *Adv. Mater.* **29** 1605900
[9] Jo J W, Yoo Y, Jeong T, Ahn S J and Ko M J 2018 *Electron. Mater. Lett.* **14** 657–68
[10] Heo J H, Lee D S, Shin D H and Im S H 2019 *J. Mater. Chem.* A **7** 888–900
[11] Bi D Q, Yi C Y, Luo J S, Décoppet J-D, Zhang F, Zakeeruddin S M, Li X, Hagfeldt A and Grätzel M 2016 *Nature Energy* **1** 16142
[12] Hu X T *et al* 2019 *Energy Environ. Sci.* **12** 979–87
[13] Yao Z, Qu D L, Guo Y X and Huang H 2019 *Org. Electron.* **70** 205–10
[14] Kim J H, Seok H J, Seo H J, Seong T Y, Heo J Y, Lim S H, Ahn K J and Kim H K 2018 *Nanoscale* **10** 20587–98
[15] Nejand B A, Nazari P, Gharibzadeh S, Ahmadi V and Moshaii A 2017 *Chem. Commun.* **53** 747–50
[16] Yang D, Yang R X, Zhang J, Liu S Z and Li C 2015 *Energy Environ. Sci.* **8** 3208
[17] Kim J G, Na S I and Kim H K 2018 *AIP Adv.* **8** 105122
[18] Cho S P, Na S I and Kim S S 2019 *Solar Energy Mater. Solar Cells* **196** 1–8
[19] Liu X Y, Yang X D, Liu X S, Zhao Y N, Chen J Y and Gu Y Z 2018 *Appl. Phys. Lett.* **113** 203903
[20] Watson B L, Rolston N, Printz A D and Dauskardt R H 2017 *Energy Environ Sci.* **10** 2500–8
[21] Rolston N *et al* 2016 *Extreme Mech. Lett.* **9** 353–8
[22] Zhang C C, Li M, Wang Z K, Jiang Y R, Liu H R, Yang Y G, Gao X Y and Ma H 2017 *J. Mater. Chem.* A **5** 2572–9
[23] Jiang J X, Wang Q, Jin Z W, Zhang X S, Lei J, Bin H J, Zhang Z G, Li Y and Liu S F 2018 *Adv. Energy Mater.* **8** 1701757
[24] Chen J Z and Park N G 2018 *Adv. Mater.* **31** e1803019
[25] Malikmammadov E, Tanir T E, Kiziltay A, Hasirci V and Hasirci N 2018 *J. Biomater. Sci., Polym. Ed.* **29** 863–93
[26] Huang S, Xiao J, Zhu Y A and Qu J 2017 *Prog. Org. Coat.* **106** 60–8
[27] Wang Y, Li M Z, Li H Z, Lan Y J, Zhou X, Li X, Hu X T and Song Y L 2019 *Adv. Energy Mater.* **9** 1900838
[28] Wu Z F, Raga S R, Juarez P E J, Yao X Y, Jiang Y, Ono L K, Ning Z J, Tian H and Qi Y B 2017 *Adv. Mater.* **70** 1703670